Stony Brook University

Bloch Oscillations of a BEC: Competition between Mean-Field Interactions and Disorder

A Thesis Presented

by

Matthias Guido Vogt

to

The Graduate School

in Partial Fulfillment of the Requirements

for the Degree of

Master of Arts

in

Physics

Stony Brook University

August 2011

Stony Brook University

The Graduate School

Matthias Guido Vogt

We, the Thesis committee for the above candidate for the Master of Arts degree, hereby recommend acceptance of the Thesis.

Dominik Schneble, Thesis Advisor
Assistant Professor, Department of Physics and Astronomy
Stony Brook University

Thomas Bergeman
Adjunct Professor, Department of Physics and Astronomy
Stony Brook University

Thomas Weinacht
Associate Professor, Department of Physics and Astronomy
Stony Brook University

This Thesis is accepted by the Graduate School.

Lawrence Martin
Dean of the Graduate School

Abstract of the Thesis

Bloch Oscillations of a BEC: Competition between Mean-Field Interactions and Disorder

by

Matthias Guido Vogt

Master of Arts

in

Physics

Stony Brook University

2011

This thesis experimentally investigates Bloch oscillations of a Rubidium-87 Bose-Einstein condensate in an disordered optical lattice. The disorder is created by superposing an additional, incommensurate optical lattice to the main lattice. Individually, collisional mean-field interactions between atoms as well as disorder both lead to a damping of the oscillations. However, we observe a competition between the two contributions, which results in an effective reduction of the disorder-induced damping due to mean-field interactions. This observation is consistent with an interaction-induced screening of the potential.

Contents

List of Figures

Acknowledgements

My year in Stony Brook is nearly over, and I am looking back at a time, which was definitely worth spending. Apart from the impressions and experiences I obtained from living and dwelling outside my home country for the first time, the work in Dominik Schneble's group was the reason for making my decision to go to the USA a good one. He welcomed me good-naturedly when I asked whether I might start in his group and turned out to be a great advisor afterwards. He always helps his students, when there is a problem or a question, and successfully motivates and encourages them without putting them under pressure. His detailed comments and suggestions where extremely helpful for me in the process of writing this thesis.

In addition to this, the good working atmosphere was also due to the other members of the group. First I want to mention Jeremy Reeves, with whom I mostly worked on Bloch oscillations and who readily answered my questions whenever I was confused about some experimental aspect. Then there is Bryce Gadway, who is always prepared to help with questions or problems concerning the machine or anything else. With his always positive attitude, it is difficult to imagine him in a bad mood. After Daniel Pertot has left, he is now the most senior student in the lab. During my time in the

group, Daniel was not working much on the machine anymore but was writing his Ph.D. thesis. However, he was always helping out competently, when help was needed. Also left has Gaku Nagashima, who gained some internal fame for his work in the lab as an undergraduate student and who was a nice person to have around in the lab. Finally, there was Marty Cohen who made valuable contributions and comments for the group during group meetings.

Besides Dominik, there were Thomas Bergeman and Thomas Weinacht in my thesis committee. I want to thank them for the very helpful feedback, which they have given me on my thesis. I experienced Tom Weinacht as a very good teacher, while I attended his class.

I also want to thank for the readiness to help of all the staff and faculty I came in contact with, which made me feel welcome in Stony Brook from the first day on.

Of course I could not write these acknowledgements without mentioning my family, most notably my parents. They have always supported me in the past and continued doing so during my stay here in Stony Brook. Whenever there was an issue in Germany that was difficult to solve from the USA, they helped me out. Thank you, some problems would have been a lot harder to solve without your help .

My year at Stony Brook and my research were supported by the DAAD and the Research Foundation of the State University of New York.

Chapter 1

Introduction

Bose-Einstein condensation was first theoretically described by Satyendra Nath Bose and Albert Einstein in 1924/1925 [1, 2]. However, an experimental realization was impossible at this time.

An important aspect towards this realization was the idea of laser cooling [3–5] and its development towards cooler temperatures, most notably sub-Doppler cooling [6, 7]. With the help of laser cooling it was possible to cool down atoms far enough into the micro-Kelvin range to trap them in an optical or magnetic trap, where they could be cooled further by evaporative cooling.

The first Bose-Einstein condensates were experimentally produced 70 years after their theoretical prediction. In 1995 the groups of Eric Cornell and Carl Wieman [8] and of Wolfgang Ketterle [9] independently and unequivocally demonstrated BECs consisting of Rubidium-87 and Sodium-23 atoms, respectively.

The condensate state of bosons reveals a whole new field of research opportunities such as the examination of vortices [10] or solitons [11]. Another

interesting area is the research on Bose-Einstein condensates in optical lattices [12–15]. A spectacular example is the superfluid to Mott insulator transition [16], in which the gas becomes strongly interacting.

In optical lattices, interactions already play an important role for single-particle effects such as Bloch oscillations [15, 17–19], which are the focus of the present work. These Bloch oscillations can be damped due to atom-atom interactions within the condensate [20, 21] or because of disorder in the lattice [22–24]. However, when both, interactions and disorder, are present simultaneously, competing effects between interactions and disorder can occur [22, 25, 26]. Repulsive interactions can screen the disordered potential of the optical lattice [27, 28] and weaken the effect of the disorder. This thesis gives a basic introduction to this issue and describes the first experimental observation of screening of disorder.

Chapter 2

Basics

In this chapter I will give a general introduction to the topic of Bose-Einstein condensates (BECs). Furthermore I describe the principle of optical lattices and how an external force leads to Bloch oscillations (BOs) of a BEC.

2.1 Bose-Einstein condensation (BEC)

As long as the distance between particles is large compared to their de Broglie wavelength, they can be approximated as being point-like (classical description). If the density of particles $n = N/V$, where N is the number of atoms and V is the volume, increases, so that the distance between them can no longer be assumed to be much greater than the de Broglie wavelength, this approximation is not valid anymore, and quantum mechanical effects have to be taken into account. At temperature T, the (thermal) de Broglie wavelength

of atoms in a gas is given by [29]

$$\lambda_T = \sqrt{\frac{2\pi\hbar^2}{mkT}}. \tag{2.1}$$

Here, $\hbar$ is the reduced Planck constant, m is the mass of the atom, k is the Boltzmann constant.

In the case of bosons, the wave function of a system of identical particles will be symmetric when particles are interchanged.

As can be seen in (2.1), the de Broglie wavelength increases with decreasing temperature. When the wavelength is large enough that the individual waves start to overlap, Bose-Einstein condensation occurs. This is the case when λ_T^3 is of the same order as the reversed density n^{-1}

$$\lambda_T^3 \sim n^{-1}. \tag{2.2}$$

In this state a macroscopic fraction of the particles is in the lowest quantum state and macroscopic quantum effects play a role. The dimensionless quantity $\rho = n\lambda_T^3$ is defined as the phase-space density [30]; in free space the critical value is $\rho = 2.612$.

For temperatures between this transition point and absolute zero there will be a mixture of non-condensed thermal atoms and those in the condensed state of a BEC (see figure 2.1). A pure BEC will appear when the temperature approaches zero.

In the case of alkali atoms [1] this phase transition happens typically at

[1] Rubidium-87 was used in the later described experiments.

around 100 nK. An increase in density also increases the transition temperature.

A very detailed introduction of the subject can be found in [29] and [31].

2.1.1 Non-interacting gas

For now I will neglect interactions between the particles and only look at non-interacting gases [29]. The influence of interactions will be taken into consideration in section 2.1.2.

Density of states

In three dimensional phase space, one free particle occupies

$$(\Delta x * \Delta p_x)(\Delta y * \Delta p_y)(\Delta z * \Delta p_z) = (2\pi\hbar)^3. \tag{2.3}$$

In momentum space, the volume of those momenta p that are smaller than a certain momentum p_0 is described by a sphere with radius p_0. Considering the energy $\mathcal{E} = p_0^2/2M$, one obtains

$$\frac{4}{3}\pi p_0^3 = \frac{4}{3}\pi(2m\mathcal{E})^{3/2}. \tag{2.4}$$

Therefore, the number of states with energies smaller than $\mathcal{E}$

$$G(\mathcal{E}) = \frac{V\frac{4}{3}(2m\mathcal{E})^{3/2}}{(2\pi\hbar)^3} \tag{2.5}$$

is just the total volume divided by the volume of a single particle.

The number of states between energies $\mathcal{E}$ and $\mathcal{E}+d\mathcal{E}$ can now be obtained by using the derivative of $G(\mathcal{E})$

$$\frac{dG(\mathcal{E})}{d\mathcal{E}}d\mathcal{E} = g(\mathcal{E})d\mathcal{E}, \tag{2.6}$$

where $g(\epsilon)$ is the density of states

$$g(\mathcal{E}) = \frac{Vm^{3/2}}{\sqrt{2}\pi^2\hbar^3}\sqrt{\mathcal{E}}. \tag{2.7}$$

In D dimensions, the result is proportional to $\mathcal{E}^{(\frac{D}{2}-2)}$. It is independent of the energy in 2 dimensions.

While this is the density of free particles, I will now discuss the case of harmonically trapped particles. Hence, consider the case of a harmonic oscillator potential with oscillation frequencies ω_i

$$V(\mathbf{r}) = \frac{1}{2}m(\omega_x^2x^2 + \omega_y^2y^2 + \omega_z^2z^2). \tag{2.8}$$

The energy levels of this potential are

$$\mathcal{E}(n_x, n_y, n_z) = (n_x + \frac{1}{2})\hbar\omega_x + (n_y + \frac{1}{2})\hbar\omega_y + (n_z + \frac{1}{2})\hbar\omega_z, \tag{2.9}$$

with non-negative integers n_i.

In order to simplify the calculations, consider the case where energies are large compared to the ground state ($\hbar\omega_i$), thus $n_i >> \frac{1}{2}$. Also the n_i may be replaced by continuous variables $\mathcal{E}_i = \hbar\omega_i n_i$. This reduces equation 2.9 to

$\mathcal{E} = \mathcal{E}_x + \mathcal{E}_y + \mathcal{E}_z$. The number of states is then [29]

$$G(\mathcal{E}) = \frac{1}{(\hbar\overline{\omega})^3} \int_0^{\mathcal{E}} d\mathcal{E}_x \int_0^{\mathcal{E}-\mathcal{E}_x} d\mathcal{E}_y \int_0^{\mathcal{E}-\mathcal{E}_x-\mathcal{E}_y} d\mathcal{E}_z = \frac{\mathcal{E}^3}{6(\hbar\overline{\omega})^3}, \tag{2.10}$$

with $\overline{\omega} = (\omega_x\omega_y\omega_z)^{1/3}$. The density of states in the case of a 3 dimensional harmonic trap is therefore

$$g(\mathcal{E}) = \frac{\mathcal{E}^2}{2(\hbar\overline{\omega})^3} \tag{2.11}$$

and

$$g(\mathcal{E}) = \frac{\mathcal{E}^{D-1}}{(D-1)!(\hbar\overline{\omega})^3} \tag{2.12}$$

in D dimensions.

Critical temperature

The Bose distribution function describes the number of particles in a certain energy state $\mathcal{E}$

$$f(\mathcal{E}) = \frac{1}{e^{(\mathcal{E}-\mu)/k_BT} - 1}. \tag{2.13}$$

Here, μ is the chemical potential, k_B is the Boltzmann constant and T is the temperature. For large energies $\mathcal{E}$, it can be approximated by the Boltzmann distribution $f(\mathcal{E}) \approx e^{-(\mathcal{E}-\mu)/k_BT}$.

Using equation 2.13 and the density of states, one can determine the number of atoms that are in an excited state

$$N_{ex} = \int_0^{\infty} d\mathcal{E}\, g(\mathcal{E}) f(\mathcal{E}). \tag{2.14}$$

In order to determine the critical temperature, which is the highest temperature at which some atoms are in the lowest quantum state (in a "'BEC-state"'), one looks at the point where all atoms are in an excited state. Consequently one sets $\mu = 0$ to obtain the greatest possible value of equation 2.14 and sets it equal to the total atom number. This way the critical temperature can be derived, depending on the kind of potential that is used and its dimensionality. For a three dimensional harmonic oscillator, the critical temperature is [29]

$$T_c = \frac{\hbar\overline{\omega}N^{1/3}}{k_B[\zeta(3)]^{1/3}}, \tag{2.15}$$

where N is the total number of atoms and ζ is the zeta function ($\zeta(3) = 1.202$).

Condensate fraction

For temperatures below the critical temperature, one can also calculate the number of excited atoms $N_{ex} = N(\frac{T}{T_c})^{\alpha}$, with α depending on the potential. By subtracting this number from the total atom number, one obtains the number of condensate atoms. For a three-dimensional harmonic oscillator ($\alpha = 3$) it is

$$N_0 = N\left[1 - \left(\frac{T}{T_c}\right)^3\right]. \tag{2.16}$$

For a rectangular box potential the power is $\alpha = 3/2$.

These are some basic parameters that can be derived without regarding the effects of interacting bosons. The next chapter will show some properties that are based on or influence by atom-atom interactions.

2.1.2 Weakly interacting gas, Gross-Pitaevskii equation

So far, interactions between particles have been neglected. Because of their influence on several of the BEC's properties, such as its shape [32], they have to be taken into consideration. For zero temperature, a scattering length that is much shorter than the spacing between particles, and high atom numbers in the condensate, Gross and Pitaevskii independently derived a nonlinear Schrödinger equation in 1961

$$i\hbar\frac{\partial\Phi(\mathbf{r},t)}{\partial t} = \left[-\frac{\hbar^2}{2m}\Delta^2 + V_{ext}(\mathbf{r}) + g\left|\Phi(\mathbf{r},t)\right|^2\right]\Phi(\mathbf{r},t). \tag{2.17}$$

A derivation and more detailed explanation of the Gross-Pitaevskii (GPE) equation can be found in [29].

The GPE is of similar appearance as the Schrödinger equation. The first term on the right side describes the kinetic energy, the second term stands for external potentials and the third covers interactions between particles. It contains the coupling constant g, which in turn depends on the scattering length a [2]

$$g = \frac{4\pi\hbar^2 a}{m}. \tag{2.18}$$

The time-independent GPE can be found by substituting the time derivative on the left hand side of the equation by the chemical potential μ

$$i\hbar\frac{\partial\Phi(\mathbf{r},t)}{\partial t} \rightarrow \mu\Phi(\mathbf{r}). \tag{2.19}$$

[2]The scattering length can both be positive or negative corresponding to a repulsive or attractive atom-atom interaction. In the case of rubidium the scattering length is positive.

In contrast to the Schrödinger equation, the eigenvalue is not generally the energy of an individual particle. Only in the case of no interactions the chemical potential is equal to the energy of the single particles.

Thomas-Fermi approximation

Let us consider the GPE in its time-independent form now and compare the kinetic energy to the interaction energy. It turns out [32] that the ratio of interaction energy to kinetic energy depends on the parameter Na/a_{ho}, where a_{ho} is the length of the harmonic oscillator trap.

For repulsive interactions, which means $a > 0$, a large enough number of atoms N leads to an interaction energy that is much greater than the kinetic energy. In that case the kinetic term can be simply neglected, which leads to the Thomas-Fermi approximation

$$\mu\Phi(\mathbf{r}) = \left[V_{ext}(\mathbf{r}) + gn(\mathbf{r})\right]\Phi(\mathbf{r}), \tag{2.20}$$

where $n(\mathbf{r}) = |\Phi(\mathbf{r})|^2$.

When the atom number is in the already experimentally realized order of about 10^5 or larger, there is hardly a difference between the Thomas-Fermi approximation and the more accurate description that includes the kinetic term [32].

Solving this equation for n and integrating, one gets the total number of atoms. By solving for μ now one obtains an expression for the chemical

potential [29]

$$\mu = \left(\frac{15^{2/5}}{2}\right)\left(\frac{Na}{a_{ho}}\right)^{2/5}\hbar\overline{\omega}, \tag{2.21}$$

where $\overline{\omega} = (\omega_x\omega_y\omega_z)^{1/3}$ is the geometric mean of the three oscillator frequencies ω_i.

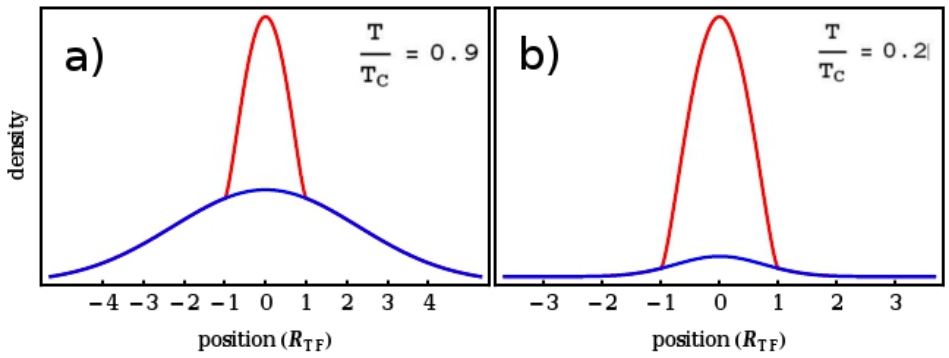

Figure 2.1: 1D cut through the density profile of a Bose-Einstein condensate: The x-axis is in units of the Thomas-Fermi radius, the y-axis is in arbitrary units. The plots are the sum of a Gauss distribution (blue curve, describes the thermal particles) and a Thomas-Fermi distribution (red curve, describes the condensate). (a) Here, the temperature is just below the critical temperature T_C. There is still a large cloud of thermal particles. (b) Due to the low temperature most of the particles are in a BEC-state.

Using the condition at the boundary of the cloud $V(\mathbf{r}) = \mu$ together with equations (2.21) and (2.8) leads to the often used Thomas-Fermi radius [29, 31]

$$\overline{R}_{TF} = (R_xR_yR_z)^{1/3} = 15^{1/5}\left(\frac{Na}{a_{ho}}\right)^{1/5}a_{ho}. \tag{2.22}$$

The Thomas-Fermi radius is a measure of the BEC's size.

2.2 Optical Lattices

2.2.1 Atoms in the presence of a laser field

When an atom is exposed to a laser field, it is affected by the oscillating electric field of the laser beam. Due to the ac Stark shift, the atom's energy levels are shifted by [13, 29]

$$\Delta E = -\frac{1}{2}\alpha(\omega)\left\langle \mathcal{E}^2(\mathbf{r},t)\right\rangle_t . \tag{2.23}$$

The electric field is denoted by $\mathcal{E}$ and $\alpha(\omega)$ is the atomic polarizability, which depends on the frequency ω of the electric field. The brackets $\langle\rangle_t$ indicate the time average of the electric field $\mathcal{E}$.

The resulting potential affecting the atom is [29]

$$V = -\frac{1}{2}Re[\alpha(\omega)]\left\langle \mathcal{E}^2(\mathbf{r},t)\right\rangle_t , \tag{2.24}$$

where $Re[\alpha(\omega)]$ is the real part of $\alpha(\omega)$.

1D lattice

Let us assume a lattice consisting of two counterpropagating beams as shown in figure 2.2. Both have the same frequency, amplitude and polarization. This results in a standing wave with an electric field

$$\mathcal{E} = \mathcal{E}_0 e^{i(kx-wt)} + \mathcal{E}_0 e^{i(-kx-wt)} = 2\mathcal{E}_0 e^{-iwt}\cos(kx). \tag{2.25}$$

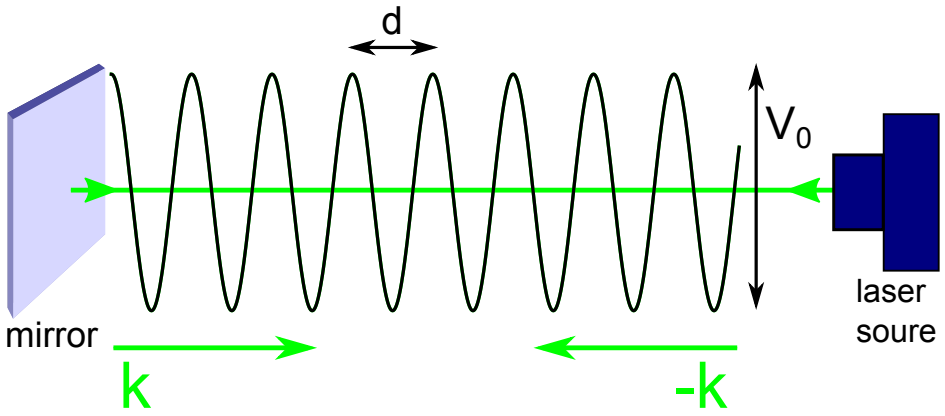

Figure 2.2: An optical lattice created by two counterpropagating laser beams with wave vector k and $-k$: In this picture a laser beam is reflected into itself by a mirror, which creates a standing wave with period d and depth V_0.

By time-averaging the squared electric field, one obtains the potential

$$V = V_0 \cos^2(kx) = V_0 \cos^2(\frac{\pi x}{d}), \tag{2.26}$$

where $d = \pi/k = \lambda/2$ is the lattice spacing and V_0 is the lattice depth. The lattice depth linearly depends on the atoms' polarizability and the intensity of the laser. It is often given in units of the recoil energy

$$E_R = \frac{(\hbar k)^2}{2m}, \tag{2.27}$$

which is the energy that an atom gains when absorbing a lattice photon.

For an arbitrary angle between both beams the lattice spacing and the potential become [29]

$$d = \frac{2\pi}{|\mathbf{k}_1 - \mathbf{k}_2|} = \frac{\lambda}{2\sin(\theta/2)} \tag{2.28}$$

and

$$V = V_0 \cos\left[(\mathbf{k}_1 - \mathbf{k}_2)\mathbf{r} + \delta_1 - \delta_2\right], \tag{2.29}$$

where θ is the angle between the two beams and $\delta_1 - \delta_2$ is their phase difference. By varying the angle θ one can control the period of the lattice and achieve values of $\lambda/2$ and higher.

A moving lattice can be created by using two beams with different frequencies. The direction of that movement is determined by $\mathbf{k}_1 - \mathbf{k}_2$ and the magnitude is [29]

$$v = \frac{\omega_1 - \omega_2}{|\mathbf{k}_1 - \mathbf{k}_2|}. \tag{2.30}$$

If the frequency difference $\omega_1 - \omega_2$ changes with time, the lattice is accelerated. This provides an alternative to accelerating the BEC in the lattice itself [14, 15, 19].

Two- and three-dimensional lattices

Optical lattices of two- or three dimensions can be achieved by using more than two laser beams with wave vectors $\mathbf{k_i}$. For two dimensions at least two independent differences $\mathbf{k}_i - \mathbf{k}_j$ produced by at least 3 beams are required. Accordingly, a three-dimensional lattice calls for at least 4 laser beams [29].

The most common approach in experiments, however, is to simply use one pair of counterpropagating laser beams for every dimension, where all pairs are orthogonal to the others. The influence of six different beams can lead to non-trivial interference patterns. This allows further adjustment of the lattice properties to the experimental needs. In order to get a simpler setup,

however, interferences between the three axes are often avoided with the help of a frequency offset of some tens of MHz. This can be achieved by using an acousto-optic modulator (AOM). Interference effects between the different directions are then shifting much faster than the atoms are oscillating and are therefore negligible (see [13]). The resulting three-dimensional potential of three independent, orthogonal pairs of beams is

$$V(\mathbf{r}) = V_0(\cos^2(kx) + \cos^2(ky) + \cos^2(kz)). \tag{2.31}$$

Further control of the lattice can be gained by adding even more beams, or adjusting the polarization and phases of the beams. Likewise the polarization can also be used to create state-dependent lattices by controlling the angle between the polarization vectors of two beams. For more details on state-dependent lattices see [33, 34].

2.2.2 Band structure

After introducing optical lattices, I will now discuss in what way they will affect the atoms in them. The principle is the same as for electrons in ionic lattices known from solid-state physics.

Consider the case of a particle moving in a periodic potential $V(\mathbf{r})$ (equation 2.31). The corresponding Schrödinger equation is

$$H\psi = \left(-\frac{\hbar^2}{2m}\nabla^2 + V(\mathbf{r})\right)\psi = \varepsilon\psi. \tag{2.32}$$

The eigenstates of this equation have the form [35]

$$\psi(\mathbf{r}) = u(\mathbf{r})e^{i\mathbf{qr}}, \tag{2.33}$$

where $\mathbf{q}$ is the quasimomentum and $u(\mathbf{r})$ has the same periodicity as the lattice potential $V(\mathbf{r})$. Equation 2.33 is normally denoted as Bloch's theorem after Felix Bloch, though in the one-dimensional case it was first derived by Floquet [35].

In order to solve equation 2.33, one can use an ansatz of describing the wave function and the potential ψ in Fourier series that have the same periodicity as the lattice. This leads to an infinite system of linear equations. If one limits the series to N terms, one gets a $N(2N+1)$-dimensional system of linear equations and $2N+1$ eigenenergies [13].

The eigenenergies are influenced by the lattice potential V_0. For a low potential $V_0 << E_R$, their structure resembles that of a free particle, while for larger potentials there are gaps between the energy bands that increase with increasing V_0 (figure 2.3).

In special cases, as in the limit of very weak or very strong potentials, an approximation of the eigenenergy can be found analytically. In the weak potential limit it is [13]

$$\frac{E(\widetilde{q})}{E_R} = \widetilde{q}^2 \pm \sqrt{4\widetilde{q}^2 + \frac{s^2}{16}}, \tag{2.34}$$

with $\widetilde{q} = q/k - 1$ and the dimensionless parameter $s = V_0/E_R$. Recall that k is the wave vector of the laser beams that form the optical lattice and q is the

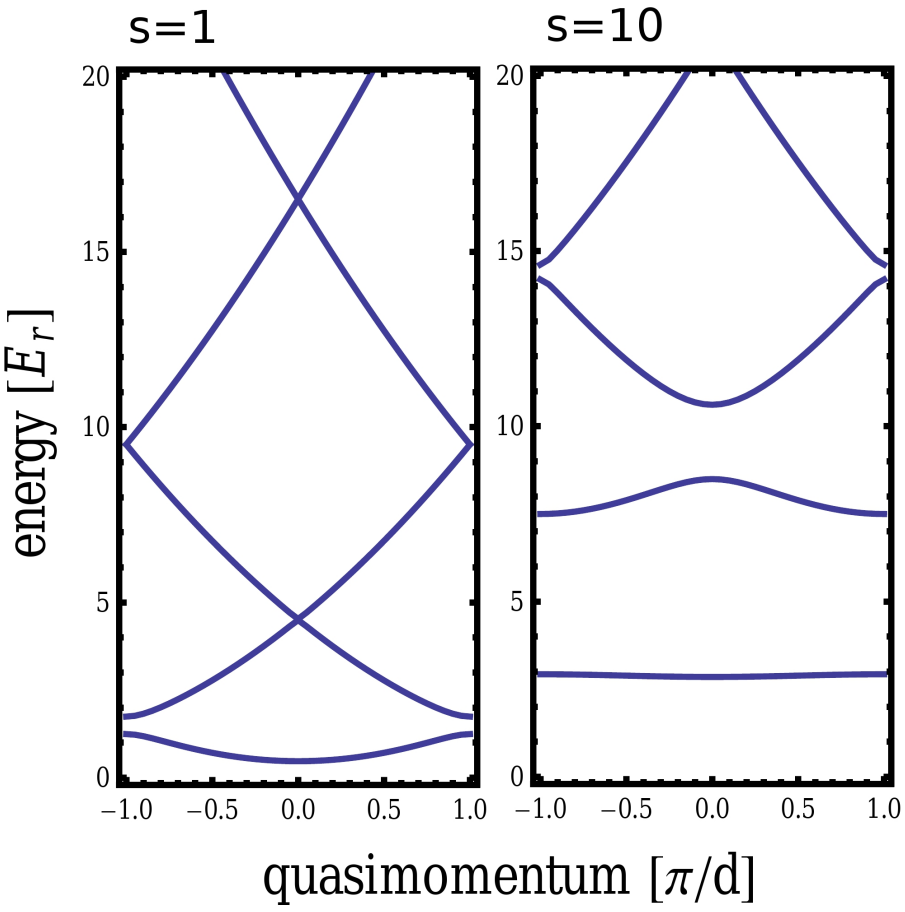

Figure 2.3: Band structure: (a) for a relatively shallow lattice potential $V_0 = E_R$ the gap between the first and the second band is small, similar to the free particle case, with no energy gaps at the end. (b) In the case of a deeper lattice $V_0 = 10 \times E_R$, the gap between the first and the second energy band is significantly broader. [Thanks to Bryce Gadway for providing a module for the calculation of the band structure.]

quasimomentum of the wave function. In case of the minus sign one gets the lowest band and plus sign gives the first excited band.

The analytical result for the limit of deep lattices is [36]

$$\frac{E(q)}{E_R} = 3\sqrt{s} - 2\frac{J}{E_R}\cos(qd), \tag{2.35}$$

$$J = \frac{4}{\sqrt{\pi}} E_R s^{3/4} e^{-2\sqrt{s}}. \tag{2.36}$$

J is the tunneling energy between the energy bands and d is the lattice spacing.

Other values of importance are the group velocity v_g and the effective mass m_{eff} of the BEC's wave packet [13]

$$v_g = \frac{1}{\hbar}\frac{\partial E(q)}{\partial q}, \tag{2.37}$$

$$m_{eff} = \hbar^2 \left(\frac{\partial^2 E(q)}{\partial q^2}\right)^{-1}. \tag{2.38}$$

2.3 Bloch oscillations

Let us consider the influence of a time-independent force F on the Bose-Einstein condensate in an optical lattice, while neglecting effects of interactions between the constituent particles for now. The force can be generated by accelerating the lattice, which will cause an acceleration of the BEC in the rest frame of the lattice. Alternatively, for a vertical oriented lattice the gravitational force [3] $F = mg$ can be used. In the presence of a one-dimensional

[3] This method was used in the experiments described later.

lattice, the resulting Hamiltonian is

$$\widehat{H} = \frac{\widehat{p}^2}{2m} + V_0 \cos^2(kx) + Fx. \tag{2.39}$$

At the beginning, the atoms are in the center of the lowest energy band (see figure 2.3). The external force F then accelerates them until they reach the edge of the Brillouin zone. Because of the band gap at this point, the atoms cannot get into the next higher band. As they cannot get to the higher band they will be reflected to the other end of the zone through Bragg reflection of the de Broglie waves at the lattice potential. Like that they will oscillate back and forth between the two edges. Accordingly, there is also an oscillation of the velocity (equation 2.37).

I will now look closer at the quasimomentum $\hbar q$. Due to the constant external force it changes as

$$\hbar \frac{\partial q}{\partial t} = F(r, t). \tag{2.40}$$

After a time of Δt the wave vector q will have changed by $F \times \Delta t/\hbar$. Because we have the periodic lattice potential, after a change of $2\pi/d$ the BEC will be in the same state as before. The time it takes, denoted as Bloch period, is

$$T_B = \frac{2\pi\hbar}{Fd}. \tag{2.41}$$

2.3.1 Landau-Zener tunneling

Whenever the atom is at the edge of the Brillouin zone there is a chance of tunneling from the lowest band to the first excited band. The chance depends on the energy uncertainty of the atoms associated with their passing through the zone edge and therefore on the external accelerating force and the band gap. The population of atoms in the lowest band decays exponentially with an estimated decay time of [18]

$$\tau = \hbar/\Gamma, \tag{2.42}$$

where

$$\Gamma = aFe^{-b/F}. \tag{2.43}$$

Here, a and b are constants that depend on the energy bands.

In order to avoid this tunneling effect, it is thus necessary to use a relatively weak force, or to increase the energy gaps between the bands by using deep enough lattice potentials.

Chapter 3

Interactions and disorder

3.1 Effect of interactions, mean-field

In chapter 2.3 interactions between atoms during Bloch oscillations have been neglected. Effectively this corresponds to a case of only a single particle. In this chapter I will take the influence of interactions into consideration.

3.1.1 Effective potential

For dilute systems the Gross-Pitaevskii equation (GPE) (equation 2.17) is a reasonable basis for calculations. Choi and Niu have used a one-dimensional GPE in [14] and applied dimensionless variables $\widetilde{x} = 2kx$, $\widetilde{t} = \frac{\hbar}{m}4k^2t$, $\widetilde{\Phi} = \Phi/\sqrt{n_0}$ and $\widetilde{V}_0 = \frac{m}{\hbar^2}\left(\frac{1}{4k^2}\right)V_0$, with n_0 being the density of the BEC to arrive at the equation

$$i\frac{\partial\widetilde{\Phi}}{\partial\widetilde{t}} = -\frac{1}{2}\frac{\partial^2\widetilde{\Phi}}{\partial\widetilde{x}^2} + \widetilde{V}_0\cos(\widetilde{x})\widetilde{\Phi} + C|\widetilde{\Phi}|^2\widetilde{\Phi}. \tag{3.1}$$

An important variable in this equation is the nonlinear coupling strength [1] [14, 15]

$$C = \frac{\pi n_0 a}{k^2 \sin^2(\theta/2)}, \tag{3.2}$$

where θ is the angle between the laser beams that generate the optical lattice.

The coupling strength is strongly influenced by the angle θ. A small angle will lead to a large lattice spacing $d = \pi/\sin(\theta/2)k$ and strong interactions. In order to minimize the effect of interactions one can use two counterpropagating ($\theta = 180°$) beams as shown in figure 2.2, for which $\sin^2(\theta/2) = 1$.

The effect of the interaction energy is to influence the potential created by the lattice. In the potential wells the number of atoms is larger, while in the regions of high potential energy, there are less atoms. In the case of repulsive interactions, the atoms will reject each other more strongly the higher the density of atoms is, which counteracts the effect of the optical lattice. This principle also plays a role in the screening of a disordered lattice described later.

The change of the total potential can be approximated by substituting the lattice potential depth $\widetilde{V_0}$ with a reduced, effective potential depth V_{eff}, depending on the coupling strength C [14]

$$V_{eff} = \frac{\widetilde{V_0}}{1 + 4C}. \tag{3.3}$$

This approximation is good as long as the effective potential depth is low ($V_{eff} << 1$), i.e. for weak external potentials.

[1] For rubidium the coupling strength is 2.6×10^{-2} [14].

3.1.2 Strongly interacting Bose gases

The Gross-Pitaevskii equation is valid in the regime of dilute and therefore weakly interacting Bose gases. Some phenomena that appear for strongly interacting BECs cannot be explained by this description. For completeness (even though this is not directly relevant for the experiments described below), I will therefore introduce the Bose-Hubbard model, that also considers quantum correlations between particles.

The derivation starts with the Hamilton operator for bosons in external potentials [12]

$$\begin{aligned} H = \int d^3r \psi^\dagger(\mathbf{r}) \left(-\frac{\hbar^2}{2m}\Delta^2 + V_0(\mathbf{r}) + V_T(\mathbf{r}) \right) \psi(\mathbf{r}) \\ + \frac{g}{2} \int d^3r \psi^\dagger(\mathbf{r}) \psi^\dagger(\mathbf{r}) \psi(\mathbf{r}) \psi(\mathbf{r}), \end{aligned} \tag{3.4}$$

where g is the coupling constant (see equation 2.18) and V_T is an external trapping potential like a magnetic trap. The last term on the right side describes the interaction potential between the atoms. It can be understood similarly as in the GPE (2.17), where the interaction strength depends on the coupling constant g and the density $|\Phi(\mathbf{r}, t)|^2$.

For only one single atom, the eigenstates of this equation are Bloch states (2.33), which can be described by a superposition of Wannier functions centered on lattice sites j,

$$w(\mathbf{r} - \mathbf{r}_j) = \frac{1}{\sqrt{N}} \sum_q e^{-i\mathbf{q}\mathbf{r}_j} \psi_q(\mathbf{r}), \tag{3.5}$$

such that

$$\psi_q(\mathbf{r}) = \frac{1}{\sqrt{N}} \sum_j e^{i\mathbf{q}\mathbf{r}_j} w(\mathbf{r} - \mathbf{r}_j). \tag{3.6}$$

With the assumption that the energies that occur in the system are small compared to the transition energy to the second band and that only the ground states of single wells are populated, the application of $\psi(\mathbf{r}) = \sum_j b_i w(\mathbf{r} - \mathbf{r}_j)$ in 3.4 leads to [12]

$$H = -J \sum_{\langle i,j \rangle} b_i^\dagger b_j + \sum_i \varepsilon_i \widehat{n}_i + \frac{1}{2} U \sum_i \widehat{n}_i(\widehat{n}_i - 1). \tag{3.7}$$

In the first term, $b_i^\dagger$ and b_i are the creation and annihilation operators. They describe the creation and annihilation of atoms in the i-th lattice site. This term therefore describes the hopping between the different sites with the hopping matrix element $J = \int d^3r w^*(\mathbf{r} - \mathbf{r}_i) \left[-\frac{\hbar^2}{2m}\Delta^2 + V_0(\mathbf{r}\right] w(\mathbf{r} - \mathbf{r}_i)$.

The operator $\widehat{n}_i = b_i^\dagger b_i$ counts the number of particles in the lattice site i and $\varepsilon = \int d^3r V_T(\mathbf{r}) |w(\mathbf{r} - \mathbf{r}_i)|^2 \approx V_T(\mathbf{r}_i)$ is the influence of the external potential on an atom in the lattice site i. Hence, the second term describes the total energy of the system due to the external potential.

The last term in equation 3.7 describes the interaction energy of all the atoms that are in the same lattice well. The parameter $U = g \int d^3r |w(\mathbf{r})|^4$ is the repulsion between two atoms in one lattice site[2].

[2]For ^{87}Rb atoms in a three-dimensional potential with $V_0 = 22E_R$ the value of the interaction constant U is about $0.28E_R$ [18].

Decay and revival of Bloch oscillations

Atom-atom interactions can lead to dynamical instability [37]. When the condensate is accelerated, its quasimomentum might reach a dynamical unstable region. That means that at a certain critical velocity the condensate's coherence is lost leading to a complex structure of the wave function [37]. Decoherence causes a decay of Bloch oscillations [18, 21].

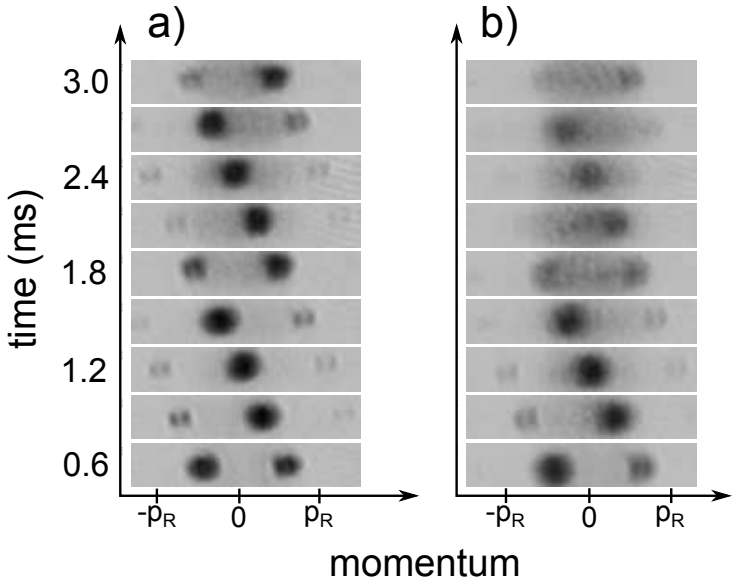

Figure 3.1: Damping of Bloch oscillations: Shown is the development of the momentum (in units of the recoil momentum p_R) in time. The atom number is about equal in both cases, but the trap confinement and therefore the density is higher for b (the trap is about three times as deep as for a). a) In the case of weaker interactions the width of the momentum distribution stays small. b) Due to collisions the coherence of the system decreases with time and the momentum distribution becomes washed out. The oscillation of the mean momentum is damped strongly.

This decay (see figure 3.1) can be understood in terms of the momentum distribution of the BEC. Due to collisions, parts of the system are scattered and different particles have different momenta at the same time, which corresponds to different oscillation phases. The initially small momentum distribution

spreads more and more and the amplitude of the mean momentum decreases.

On the other hand for a sufficiently strong external force even periodic revivals of Bloch oscillations have been predicted for certain conditions. These revivals are a quantum many-particle effect and based on the finiteness of the interaction constant U and the atom number [38].

3.2 A disordered lattice

In solid state physics, Bloch oscillations of electrons in crystal structures will decay in times that are much shorter than an oscillation period. The reason for this are imperfections in the lattice structure like impurity atoms or phonons that disturb the otherwise periodic potential and lead to scattering of the electrons. In contrast to this, optical lattices created with laser beams have a perfectly periodic potential. It is, however, possible to add a controlled disorder potential to the optical lattice in order to analyze its effect on the damping of Bloch oscillations. The first experimental measurements on the decay of Bloch oscillations in a disordered lattice have been reported by Drenkelforth et al. in 2008 [24].

There are several ways to create such a disordered lattice potential. One possibility is to add a different kind of atoms [39] as impurities. For example they can be in a different hyperfine state [40] or be of another species, e.g. fermions [41]. The impurities are trapped in a deep lattice that does not or only weakly affect the other atoms. If the number of impurity atoms is low enough that they occupy only some of the lattice sites, they will create

random potential peaks on which the other atoms are scattered due to atom-atom collisions.

Because of the scattering, interference effects like interference between the incident wave and a wave scattered back from a disordered part occur [23] and the decoherence of the system increases. The decay of the wave function also leads to a decay of its Bloch oscillations. For very strong disorder, this can lead to a complete stop of the wave and to a localization of the particles inside the lattice. The effect is named "Anderson localization" after P. W. Anderson, who proposed it for lattices in the context of solid state physics [42].

A second possibility is to apply an additional, incommensurate lattice of different wavelength [43]. This setup is referred to as bichromatic lattice and has been used in the experiments described in 5. I will explain it further in section 3.2.1.

Other ways are to use speckle patterns [44, 45] or inhomogeneous magnetic fields [46, 47]. To create speckle patterns, laser light is either transmitted through a diffuse medium or reflected from a rough surface [23]. Inhomogeneous fields can be found in the vicinity of microchips due to fabrication imperfections. Small fluctuations of an inhomogeneous magnetic field close to the Feshbach resonance (see e.g. [48, 49]) generate spatial fluctuations in the scattering length that characterizes atomic interactions. Effectively the disorder that is achieved in this way is a disorder of the interaction strength, not of the optical lattice [23].

Because of the disorder, the total external potential affecting the bosons

is in one dimension

$$V(x) = \frac{m\omega^2 x^2}{2} + sE_R \cos^2(kx) - Fx + V_{dis}(x). \tag{3.8}$$

The first term stands for the harmonic trap, the second term denotes the optical lattice with s being the lattice depth in terms of the recoil energy E_R and the third term is due to the external force that accelerates the atoms. The last term finally is the disorder potential V_{dis}, which causes a damping of the Bloch oscillations.

3.2.1 A bichromatic lattice

Combining two optical lattices with different wavelengths creates a bichromatic lattice with the potential

$$V(x) = s_1 E_{R1} cos^2(k_1 x) + s_2 E_{R2} cos^2(k_2 x). \tag{3.9}$$

The parameters $s_i = V_i/E_{Ri}$, $E_{Ri} = h^2/(2m\lambda_i^2)$ and $k_i = 2\pi/\lambda_i$ all depend on the wavelengths of the lattices. The second lattice, described by the second term in equation 3.9 acts as the disorder potential V_{dis}.

Because a bichromatic lattice is based on the superposition of two discrete wavelengths, it cannot really be a disordered potential with random impurities but will always have a periodic structure. This is called a quasiperiodic potential. For finite sized systems, however, they are suitable as long as their wavelengths are approximately incommensurate. Incommensurability means

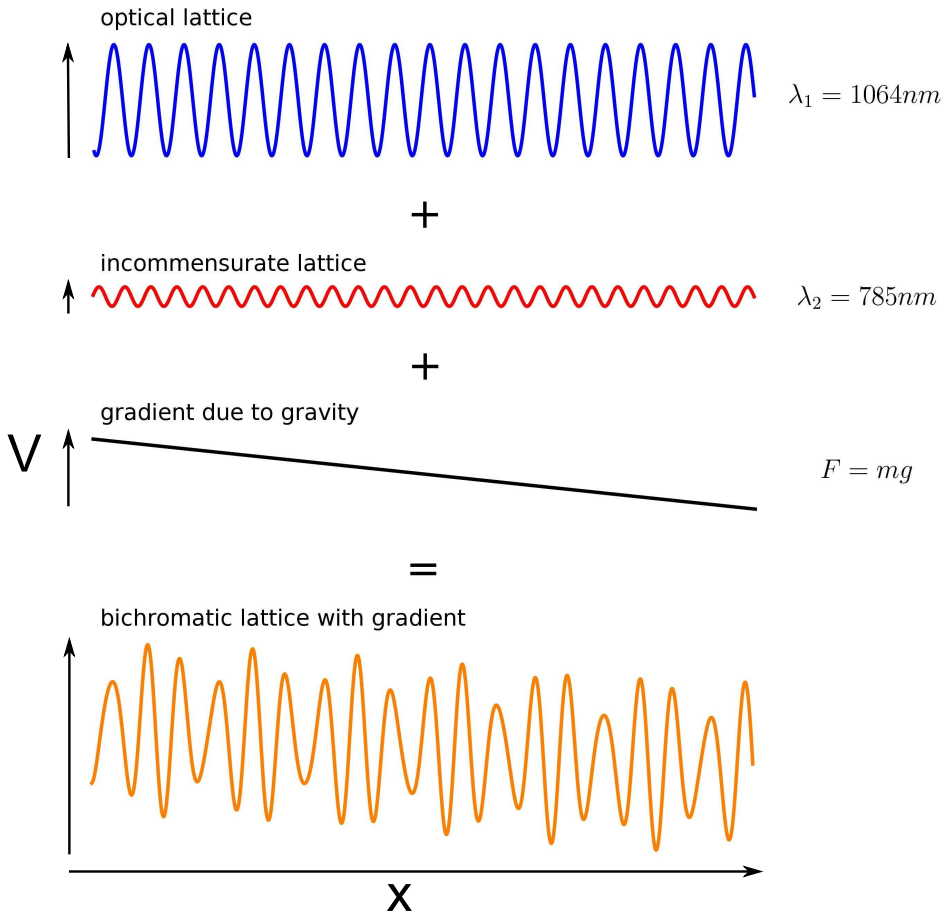

Figure 3.2: A tilted bichromatic lattice: The first potential (blue) is the regular optical lattice. In order to obtain disorder, a second lattice (red) with lower lattice depth and an incommensurate wavelength is added. The accelerating force needed for Bloch oscillations is provided by gravity. It is a linear gradient. The orange potential is the tilted bichromatic lattice resulting from a superposition of all potentials.

that the ratio of both wavelengths is an irrational number, which is experimentally not feasible because the precision for measuring the wavelength is limited. But as long as the ratio is far enough from an integer or half-integer [22] that the periodicity of the bichromatic lattice is greater than the size of the measured system, the lattice can be considered to be effectively incommensurate [23].

If the potential depth of the disordering lattice is much smaller than that of the main lattice, the height of the potential barriers between the wells can be assumed to be approximately constant. In this case, the main effect of the second lattice is to induce a non-periodic shift of the potential energy's minima [23].

In order to induce Bloch oscillations, an additional external force is needed. It can be provided by gravity, which then adds the additional potential term $V_G = mgx$ to equation 3.9.

3.3 Interplay between disorder and interactions

If applied independently, both atom-atom interactions and disorder cause a decay of Bloch oscillations. However, if both interactions and disorder are present simultaneously, the effects might weaken or even annihilate each other [22, 25]. For a lattice with a fixed amount of disorder, the interaction strength can be controlled e.g. via Feshbach resonance or the density of the condensate.

Consider a disordered lattice and noninteracting particles or a very dilute condensate with significantly damped Bloch oscillations. When adding interactions or increasing the density, this can give rise to a screening of the disordered lattice [25, 27, 28]. The condensate wave function is attracted to those places of the lattice with lowest energy, i.e. the minima. We recall that the depth of these wells varies in a disordered lattice. Accordingly, more atoms assemble in the deeper minima than in the more shallow minima. The accumulated atoms repel each other because of their repulsive interaction and the strength of this repulsion depends on the density of the condensate. The deeper the lattice, the denser the condensate and the stronger is the repulsive potential caused by atom-atom interactions. On account of this, the deepest minima are "cut off", the lattice becomes a little more shallow and the effects of disorder are smoothed out [28] (see figure 3.3). Of course this happens not in one sudden step, but the interplay of interactions and disorder leads to the disordered potential converging to the screened potential.

The screening leads to a delocalization of the particles in the lattice [26]. Increasing the interaction strength also increases the effect of the dynamical screening. At first, locally coherent fragments of BEC arise and for further increase of the strength the entire system reaches a coherent state.

While the coherence of the system is strengthened the damping of Bloch oscillations is weakened. This works up to a certain point where the influence of decoherence induced by interactions becomes stronger than the influence of the dynamical screening. From here, a further increase of interaction strength will again lead to more damping [22].

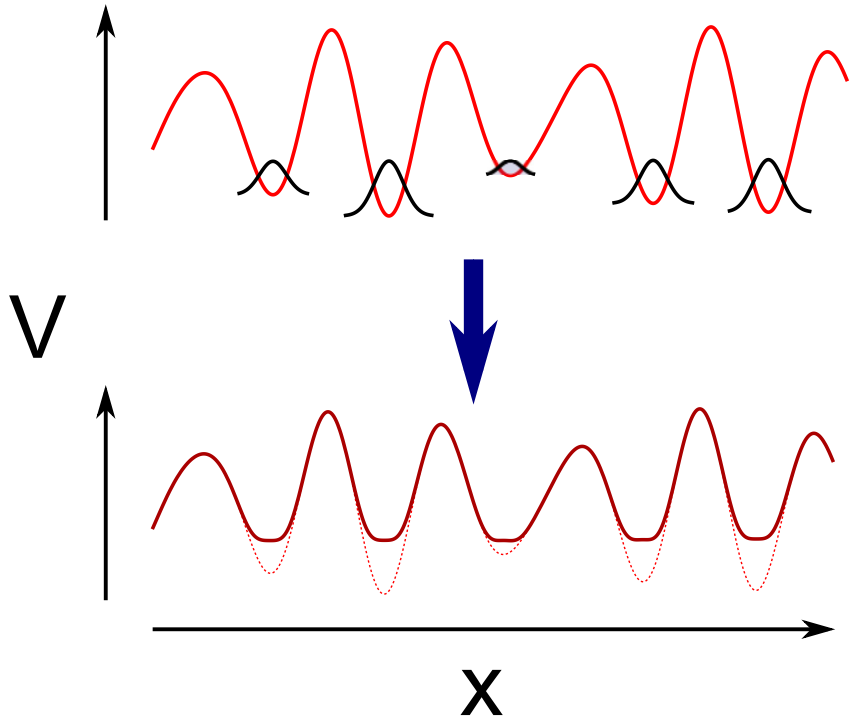

Figure 3.3: Schematic illustration of the combined effects of disorder and interactions: On top is a disordered lattice (red) and the repulsive potential caused by atom-atom interactions (black). The deeper the lattice wells are, the greater is the number of atoms in it and their interaction strength. This leads to a screened effective potential, in which the deepest minima are cut off. The disordered lattice is smoothed out at the bottom.

In conclusion, it should be possible to counter the effect of a disordered lattice by tuning the atom-atom interactions. Experimental results of this procedure are described in chapter 5.

Chapter 4

Experimental Setup

A detailed description of the experimental steps that lead to the production of a BEC in our apparatus are described in [50–53].

In brief, ^{87}RB atoms are first slowed down and collected in a magneto-optical trap (MOT). For that purpose a frequency stabilized diode laser excites the atoms from the $5^2S_{1/2}, F = 2$ hyperfine state to the $5^2P_{3/2}, F' = 3$ state. Most of the atoms will decay back to the $F = 2$ state but a few decay over the F'=2 state into the F=1 state. In order to minimize losses they are pumped back into the $F = 2$ state by a repump laser. An extensive introduction on laser cooling is given in [54].

After the atoms are trapped in the MOT, they are optically pumped to the $|F = 1, m_F = -1\rangle$ hyperfine ground state. Subsequently the atoms are captured in a magnetic quadrupole trap and mechanically transfered into an ultra-high vacuum (UHV) chamber, where the experiments take place.

The final step is now to cool the atoms down by evaporative cooling to the order of about 100nK and obtain Bose-Einstein condensation.

4.1 Optical lattice and dipole trap

In this section I will give a general overview of the optical lattice setup (see 4.1) that is used in our group. An elaborate description of the lattice configuration and its properties can be found in [33].

First, there is a three-dimensional lattice, which is created by three orthogonal laser beams with their minimum waist focused on the BEC and a wavelength of 1064nm. Therefore the lasers are far red detuned from any transitions of ^{87}Rb and the hyperfine states, in which the atoms are, can be neglected. The 1064nm-lattice is thus state-independent. We note that, for the experiments described in chapter 5, only a one-dimensional lattice (in vertical direction) was used.

Two of the beams that span a plane parallel to the ground (xy-plane) are alternatively used as crossed optical dipole trap (XODT), where each laser beam can individually form an optical dipole trap (referred to as ODT1 and ODT2). This XODT is used in the later described experiments. The advantage of such an optical trap over a magnetic trap is the independence of the atom's magnetic state induced by the Zeeman effect. Hence, a strong influence of the Zeeman effect on the energy is avoided. Also the application of homogeneous magnetic fields is possible that stands in contradiction to the inhomogeneous field of a magnetic trap.

In order to use these laser beams as optical lattice, they are reflected back by a mirror and superposed with the incoming beam to a standing wave. The intensity of the reflected beams and with it the depth of the lattices can

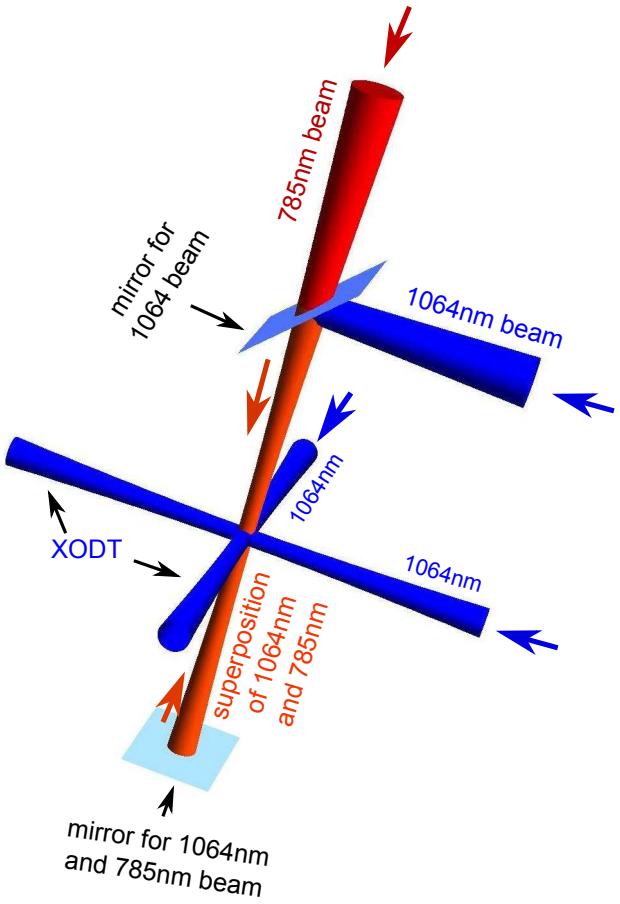

Figure 4.1: Three-dimensional view on the lattice configuration: In vertical direction a bichromatic lattice can be set up by using both the 1064nm and the 785nm beam. The beams are reflected by a mirror at the bottom. The 1064nm beams in horizontal direction are used as crossed optical dipole trap. Alternatively they can also form an three-dimensional optical lattice together with the vertical beam if they are retroreflected with mirrors.

be controlled by AOMs, which are placed in front of the mirrors. In particular this allows to precisely control the speed at which the lattice is ramped up. If the lattice is ramped up too quickly, the process will disturb the BEC and induce decoherence. The time it takes until coherence is recovered is about as long as the tunneling time between the lattice wells but at this point a considerable amount of the condensate would be lost [13].

The beams in the xy-plane are detuned by 20MHz from each other and by 10MHz from the third beam, which is directed parallel to gravity (z-direction) [33]. Thus, interference effects between the orthogonal beams are avoided.

In addition to this three-dimensional lattice a one-dimensional lattice can be added in z-direction. With a wavelength of 785nm it is in between the D2 (780.2nm) and the D1 (795.0nm) transition line of ^{87}Rb [55]. Because of this, the hyperfine structure of the atoms is no longer irrelevant, and the lattice is state-dependent (this feature is used in other experiments done in our laboratory). Depending on whether the transitions are blue or red detuned the atoms experience an attractive or repulsive force. This force also depends on the amount of the detuning. As a consequence of the two different transition lines there may also be a competition between the attractive force of one line and a repulsive force of the other one. Ultimately it is even possible that they cancel out each other, leaving the atoms unaffected.

During the experiments we are operating the atoms in the $|F = 1, m_F = -1\rangle$ or $|F = 2, m_F = -2\rangle$ hyperfine states. By controlling the beam polarization with a $\lambda/4$ plate the effect on the two kinds of atoms can be adjusted. Effectively this means that the lattice depth for atoms in different states is control-

lable. It is possible that one kind is not or only weakly affected by the lattice while the other one is strongly affected. For the experiments on BOs, where we operate in the $|F = 2, m_F = -2\rangle$ hyperfine state, the state-dependence is not relevant, though.

Kapitza-Dirac diffraction and dipole oscillations

The depth of the lattice can be determined by using Kapitza-Dirac diffraction [56]. While the BEC is held in the trap, the lattice is switched on for a short time. The condensate wave function is now diffracted from the lattice and a picture of the diffraction pattern is taken. The population of the n-th order of diffraction depends on the lattice depth and the time it was switched on. For a description of this method see [33, 57].

The trap frequency of the XODT is found by applying dipole oscillations. The oscillations are induced by a short magnetic pulse that kicks the atoms out of their rest position in the trap. Hereupon they oscillate inside the trap. After some time the trap is switched off and after a time of flight (TOF) of a few milliseconds a picture is taken. The position of the atoms marks their momentum at the time they were released from the trap. By switching the trap off at consecutive times one can obtain the trap frequency.

4.2 The route to Bloch oscillations

We start at the point where the atoms are trapped in the crossed optical dipole trap (XODT) and are in the $|1, -1\rangle$ hyperfine state. The two horizontal

1064nm beams are used for the XODT. As the next step, the atoms are now transferred with a Landau-Zener sweep (see section 4.2.1) into the $|2,-2\rangle$ state. In this state the atoms are fully affected by the 785nm lattice, which is used as disordering lattice.

In order to compensate for gravity, a magnetic field gradient is added, which levitates the BEC. Later it is possible to vary the amount and the direction of the external force that induces Bloch oscillations by adjusting this gradient.

As the next step, we can tighten or expand the levitated XODT, which determines the density and thus also the interaction strength. Consecutively, we now ramp up our lattice adiabatically over a time of 50ms. This ensures that no nonadiabatic disturbance of the BEC occurs. If we want an incommensurate lattice, we can ramp up both vertical lattices. The wavelengths used for the experiment were 1064nm and 785.7nm. Otherwise we can use either of them for an undisturbed optical lattice.

For Bloch oscillations, we now need an external force, which we achieve by switching off the magnetic field gradient within less than 0.2ms. So, gravity is the driving force for the oscillations. It creates an energy offset of $0.56E_R$ between neighboring lattice sites. The corresponding oscillation period is $T_B \approx$ 0.88ms.

After some time, in which the atoms oscillate in the optical lattice, the dipole trap and the lattice are switched off and the atoms are released to a free fall. After a time of flight of 18 ms, an image of the BEC is taken. Here, the vertical position is proportional to the velocity of the atoms at the time of

their release.

By running this sequence for several times and changing the oscillation time, we get a series of consecutive images. We then calculate the mean velocity for each image and plot the velocities versus time.

In order to find out how many pixels in the image correspond to the recoil velocity, one can size the distance between two diffraction peaks. Therefore two Gaussian distributions are plotted that sit on top of a third one. The recoil velocity in terms of image pixels can be determined from the distance between the centers of the first two Gaussian distributions.

4.2.1 Hyperfine-state transfer

Quite generally, an atom can absorb a photon and be transfered to a higher energy level, if the frequency of the photon coincides with the energy difference of the two states $\omega = (E_2 - E_2)/\hbar$. Likewise a photon with that frequency can stimulate the transition of an atom from the higher state to the lower state, which causes the emission of a photon. The chance of absorption and emission is smaller, if the frequency of the photon ω differs from the transition frequency ω_0. This difference $\Delta = \omega_0 - \omega$ is called detuning.

In a coherent driving field the probability of an electron in a two-level system to be in one state will change over time with the generalized Rabi frequency

$$\Omega_R = (\omega_R^2 + \Delta^2)^{1/2}, \tag{4.1}$$

where ω_R is the ordinary Rabi frequency at zero detuning.

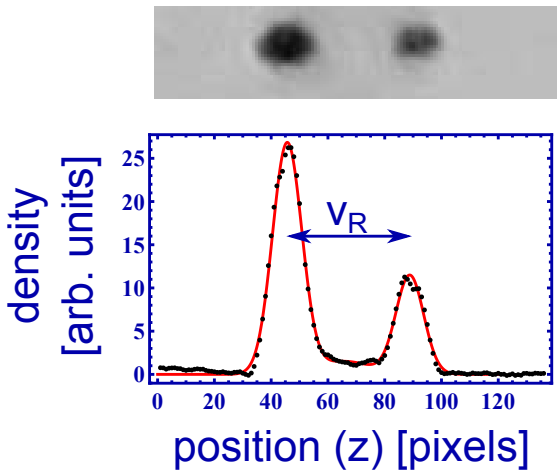

Figure 4.2: On top is the experimental image that is taken after TOF. At the bottom is a plot of the density distribution. The black points are data and the red curve is a fit consisting of two Gaussian distributions on top of a third Gaussian. The recoil velocity is determind through the distance between the peaks.

For an atom, which is initially in the ground state E_1, the probability to be in the excited state E_2 is

$$P_2 = \left(\frac{\omega_R}{\Omega_R}\right)^2 \sin^2\left(\frac{\Omega_R t}{2}\right). \tag{4.2}$$

A derivation of this formula can for example be found in [58].

It is thus possible to transfer an electron into an excited state by applying a pulse with the right frequency for a certain amount of time.

In order to hit the right frequency, it is beneficial to vary the frequency of the laser pulse over time. This is especially necessary if there are several atoms in an inhomogeneous magnetic field. Because of the Zeeman effect their transition varies spatially. This process is called a Landau-Zener sweep. For our experiments we microwave radiation to drive transitions between hyperfine

states.

Chapter 5

Experimental data

In this chapter I will present the results obtained from the experiments.

The Bloch oscillations are generally fitted with an approximation of the velocity function. Specifically, we use the derivative (see equation 2.37) of a Taylor expansion of the first energy band and a Gaussian decay envelope

$$v(t) = Ae^{-\frac{t^2}{\tau^2}} \left(B_1 \sin(\frac{2\pi t}{T_B} + \phi) - B_2 \sin(\frac{4\pi t}{T_B} + \phi) + B_3 \sin(\frac{6\pi t}{T_B} + \phi) \right), \tag{5.1}$$

where A is the amplitude, τ is the decay time, B_i are fixed parameters ($B_1 = 0.5826$, $B_2 = 0.1506$ and $B_3 = 0.0414$), ϕ is a phase shift, and T_B is the oscillation period. The impact of the parameter B_3 is less than a tenth of the first one (B_1). Further elements of the expansion are therefore neglected. The phase shift may be caused by a possible non-zero initial velocity that could for example be due to the short time it takes to switch off the gravity compensating gradient.

The Gaussian envelope fits best for to the experimentally obtained data

and is justified by the assumption of a linear increase of the momentum distribution in time that leads to a Gaussian envelope [24, 59].

5.1 Bloch oscillations (BOs) for weak interactions

First, we measured Bloch oscillations up to a time of 31ms, which corresponds to about 35 oscillations (see figures 5.1 and 5.2, $T_B \approx 0.88$ms). For this purpose, we used the 1064nm lattice without disorder and with a relatively shallow trap. The images were taken from 0 to 3, 6 to 9, 12 to 15, 18 to 21, 24 to 26, and 30 to 31 milliseconds in steps of 0.2ms. The first part (0-3ms) was repeated three times to gain a higher precision. For each of these images the mean velocity was determined by averaging over the whole picture. Then we calculated again the mean of the mean velocities obtained from three images.

The mean velocities are finally plotted versus the time and fitted with equation 5.1. This is the general procedure that we also used for the following analyses.

As can be seen in figure 5.1, there is a light decay of the Bloch oscillations. Because the oscillations are still visible very well at the end, the measurement over longer times should be possible. The decay time is (32.2 ± 0.3)ms, which corresponds to about 36.6 Bloch periods.

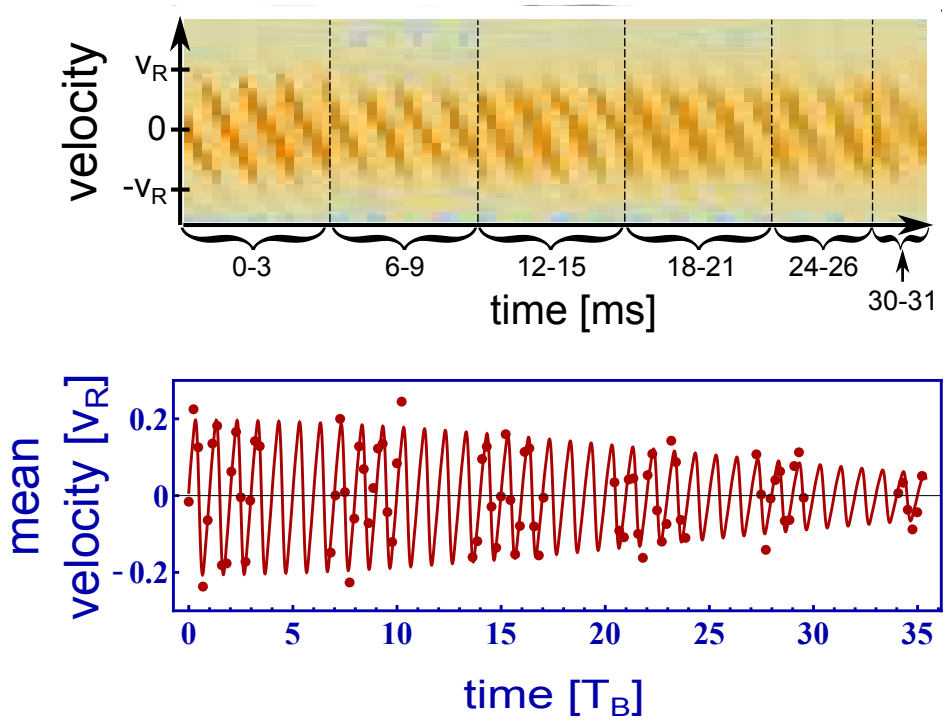

Figure 5.1: Bloch oscillations for weak interactions ($\mu \approx 0.1E_R$): Above are density plots of the consecutive images, where the oscillation is already clearly visible. The time evolution goes from left to right and the black bars denote the cuts in the imaging, where we jumped to later times (see description in the text). One can nicely see the BEC's being Bragg reflected at the edge of the Brillouin zone. At the bottom are plotted the mean velocities in units of the recoil velocity vs the time in units of the oscillation period ($T_B \approx 0.88$ms). The solid line is the fit function from equation 5.1. For a larger picture of the first part see figure 5.2

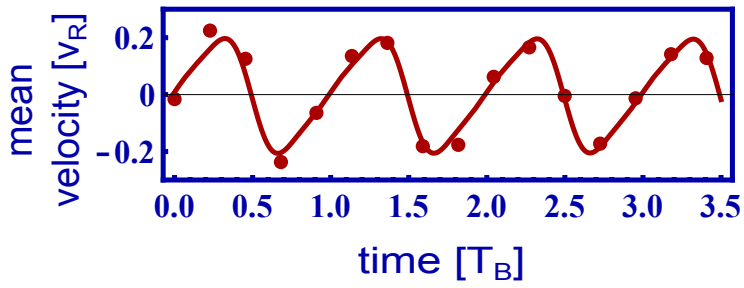

Figure 5.2: To help appreciate the quality of the fit to the data points, an extended view of figure 5.1's first part is shown here.

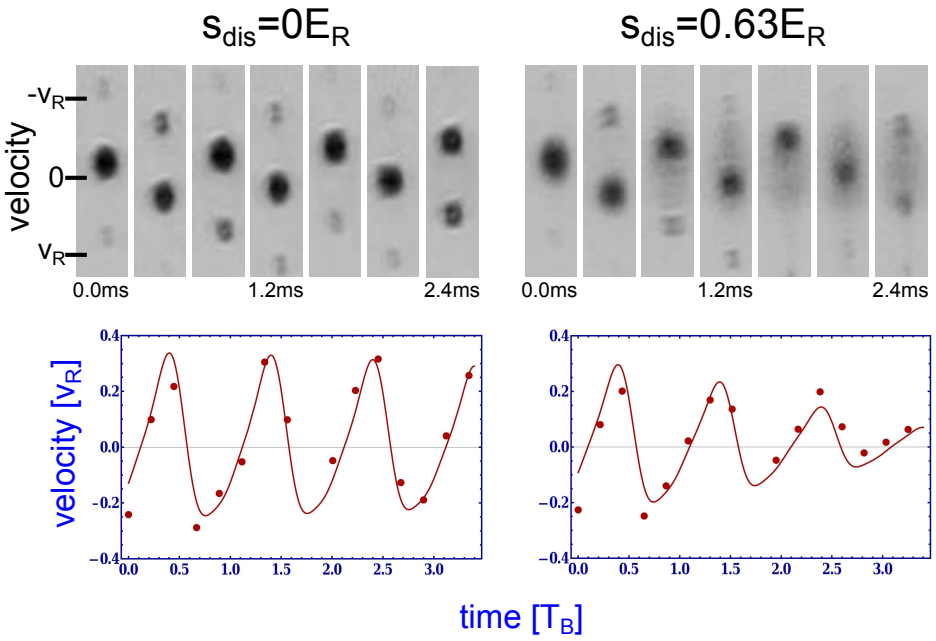

Figure 5.3: Effect of disorder on the lifetime of BOs: On top are the experimental images that have been taken after a TOF of 18ms. It is noticeable that at later times in the disordered lattice they are washed out. The plots show data together with their fit functions (solid lines). The damping rate is considerably increased in the disordered lattice ($0.37T_B^{-1}$; compared to $0.11T_B^{-1}$ for $s_{dis} = 0E_R$).

5.2 Effect of a disordered lattice

In addition to our main optical lattice ($s_1 = 3$, λ_1 =1064nm), we applied a second lattice with lower depth (varying between $s_2 = 0$ and $s_2 = 1$) and a wavelength (λ_2 =785.7nm) that is approximately incommensurate to the one of our main lattice.

For all the measurements with a disordered lattice, we took three sets of Bloch oscillations for each disorder depth and each interaction strength. The single shots were taken in random order to avoid systematic errors that might arise from drifts of our experimental setup during the runs, although we did not notice any dependence of that kind. This method assures that we are insensitive towards trivial damping effects that are based on heating of the machine or other drifts during the run. We then determined the damping rate by fitting the function in equation 5.1 to the oscillations and taking the mean of the three runs.

As is shown in the example in figure 5.3 for weak interactions, an added disorder leads to a dephasing of the Bloch oscillations. The increased damping is clearly visible. Also, the image of the BEC becomes washed out after less than two milliseconds, while the peaks of the non-disorder case are still very well defined at this time. The damping rate in this example is about $0.11T_B^{-1}$ and $0.37T_B^{-1}$ for the pure and the disordered lattice, respectively.

The asymmetry of the plot functions is due to the form of the first energy band. It is bent towards a horizontal position at the egde of the Brillouin zone, which also leads to the band gaps. This effect increases with increasing lattice

depth and leads to symmetric oscillations of the velocity. For shallow lattices, however, the fact that the energy band is bent just at the edge of the zone leads to asymmetry of the velocity function that is the derivative of the energy band with respect to the quasimomentum.

5.2.1 Competition between mean field and disorder

Dependence on the disorder depth

To clarify the dependence of the damping rate on the disorder lattice depth, we took measurements for several disorder depths. The results are plotted in figure 5.4 for three different interaction strengths (characterized by the chemical potential). In all three cases the damping rate seems to depend linearly on the disorder depth.

Remarkable at this place is the difference of the slope in the weakly interacting case ($\mu = 0.07$) and for stronger interactions. For zero disorder depth the damping increases with interaction strength. But when the disorder is increased, the damping rate of the weakly interacting BEC's BOs increases much faster than the other ones. At a disorder depth of around $0.4E_R$ the damping is even stronger than for stronger interactions.

This is an indication that dynamical screening takes place. It seems that the stronger interactions diminish the effect of the disorder potential and keep the damping rate relatively stable while the disorder is increased. Of course the lack of more data points and more different interaction strengths between the weak one ($\mu = 0.07E_R$) and the higher ones ($\mu \geq 0.28E_R$) does not allow

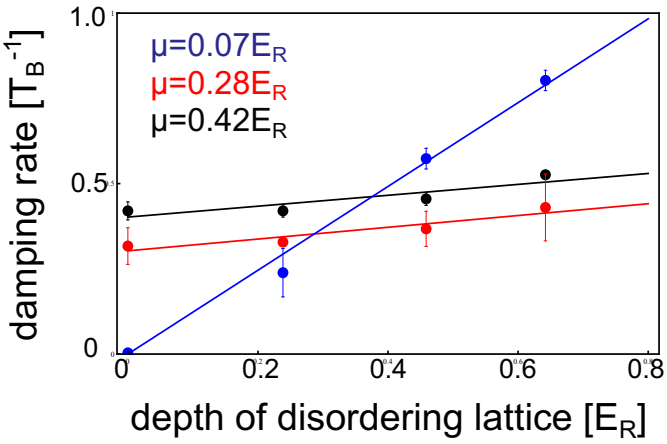

Figure 5.4: Damping of BOs in a disordered lattice for varied disorder: When the disorder depth is increased the damping rate increases also linearly. However, the slope is much steeper if the atom-atom interactions are very weak ($\mu = 0.07E_R$). The error bars represent the standard deviation resulting from taking the arithmetic average of three measurements for each point.

to draw assured conclusions at this point. In the next chapter I present the measurement of damping rates at more different interaction strengths for a disorder depth of $0.56E_R$.

Dependence on the chemical potential

We took another series of measurements where we held the disorder depth constant and varied the interaction strength (figure 5.5). The depth of the incommensurate lattice was at $s_2 = 0.56E_R$, which is in the regime where the damping rate is smaller for stronger interactions than for very weak interactions (figure 5.4).

Due to the disorder, the minima of the optical lattice are shifted between $0E_R$ and $0.56E_R$. The average shift is therefore $\langle \Delta E \rangle \approx 0.28E_R$.

It is very obvious that the damping rate decreases if interactions are applied. This goes up to a chemical potential of about $\mu = 0.26E_R$. At this point the damping rate starts to increase for further increase of the interaction strength. The turning point stands in very good agreement with the average shift of the optical lattice. Because there are more atoms in the deeper lattice sites, the interaction strength is also stronger than on average, while in the more shallow sites it is weaker. Comparing the average values of interaction and chemical potential is thus a tempting way to explain the position of the minimum in the damping rate versus interaction strength plot.

Hence, this result strongly suggests that a dynamical screening takes place. The trend of the plot also is in qualitative agreement with numerical calculations that have been done previously [22].

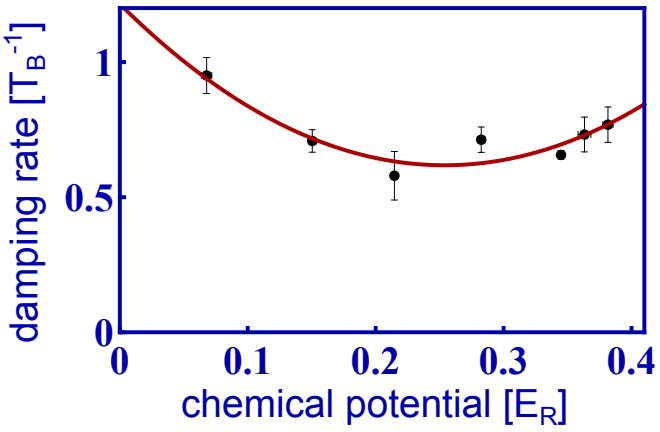

Figure 5.5: Damping of BOs in a disordered lattice ($s_1 = 3E_R$, $s_2 = 0.56E_R$)versus interaction strength: Shown are the data points with a parabolic fit ($f_{par} = a(\mu - b)^2 + c$, where a, b and c are free parameters). The minimum of the parabola is at $\mu \approx 0.26E_R$. The decrease of the damping at the beginning is indicative of dynamical screening.

Chapter 6

Conclusion

We have observed Bloch oscillations of a Rubidium-87 Bose-Einstein condensate in an optical lattice. Furthermore we have seen a damping of these oscillations, which is caused by repulsive atom-atom interactions as well as by disorder in the optical lattice.

A competing effect between interactions and disorder emerges when both are applied at the same time. The repulsive effect of the interactions works against the attractive force of the lattice wells and lifts the minima of the lattice, effectively smoothing the disordered structure of the lattice.

The damping due to disorder is therefore reduced until the interaction strength is equally strong as the disorder.

Bibliography

[1] S. N. Bose, Plancks Gesetz und Lichtquantenhypothese, *Zeitschrift für Physik* **26**, 178 (1924).

[2] A. Einstein, Quantentheorie des einatomigen idealen Gases, *Sitzungsberichte der Preussischen Akademie der Wissenschaften* **1**, 3 (1925).

[3] D. Wineland and H. Dehmelt, Proposed $10^{14}\ \Delta\, nu < \nu$ Laser Fluorescence Spectroscopy on Tl+ Mono-Ion Oscillator III (side band cooling), *Bull. Am. Phys. Soc.* **20**, 637 (1975).

[4] T. W. Hänsch and A. L. Schawlowa, Cooling of gases by laser radiation, *Optics Communications* **13**, 68 (1975).

[5] D. J. Wineland, R. E. Drullinger, and F. L. Walls, Radiation-Pressure Cooling of Bound Resonant Absorbers, *Phys. Rev. Lett.* **40**, 1639 (1978).

[6] P. D. Lett, R. N. Watts, C. I. Westbrook, W. D. Phillips, P. L. Gould, and H. J. Metcalf, Observation of Atoms Laser Cooled below the Doppler Limit, *Phys. Rev. Lett.* **61**, 169 (1988).

[7] J. Dalibard and C. Cohen-Tannoudji, Laser cooling below the Doppler limit by polarization gradients: simple theoretical models, *J. Opt. Soc. Am. B* **6**, 2023 (1989).

[8] M. H. Anderson, J. R. Ensher, M. R. Matthews, C. E. Wieman, and E. A. Cornell, Observation of Bose-Einstein Condensation in a Dilute Atomic Vapor, *Science* **269**, 198 (1995).

[9] K. B. Davis, M. O. Mewes, M. R. Andrews, N. J. van Druten, D. S. Durfee, D. M. Kurn, and W. Ketterle, Bose-Einstein Condensation in a Gas of Sodium Atoms, *Phys. Rev. Lett.* **75**, 3969 (1995).

[10] S. Stock, B. Battelier, V. Bretin, Z. Hadzibabic, and J. Dalibard, Bose-Einstein condensates in fast rotation, *Laser Physics Letters* **2**, 275 (2005).

[11] T. Tsuzuki, Nonlinear waves in the Pitaevskii-Gross equation, *Journal of Low Temperature Physics* **4**, 441 (1971).

[12] D. Jaksch, C. Bruder, J. I. Cirac, C. W. Gardiner, and P. Zoller, Cold Bosonic Atoms in Optical Lattices, *Phys. Rev. Lett.* **81**, 3108 (1998).

[13] O. Morsch and M. Oberthaler, Dynamics of Bose-Einstein condensates in optical lattices, *Rev. Mod. Phys.* **78**, 179 (2006).

[14] D.-I. Choi and Q. Niu, Bose-Einstein Condensates in an Optical Lattice, *Phys. Rev. Lett.* **82**, 2022 (1999).

[15] M. Cristiani, O. Morsch, J. H. Müller, D. Ciampini, and E. Arimondo, Experimental properties of Bose-Einstein condensates in one-dimensional

optical lattices: Bloch oscillations, Landau-Zener tunneling, and mean-field effects, *Phys. Rev. A* **65**, 063612 (2002).

[16] B. G. Levi, From Superfluid to Insulator: Bose-Einstein Condensate Undergoes a Quantum Phase Transition, *Physics Today* **55**, 18 (2002).

[17] M. Ben Dahan, E. Peik, J. Reichel, Y. Castin, and C. Salomon, Bloch Oscillations of Atoms in an Optical Potential, *Phys. Rev. Lett.* **76**, 4508 (1996).

[18] A. R. Kolovsky and H. J. Korsch, Bloch oscillations of cold atoms in optical lattices, *International J. of Mod. Physics* **18**, 1235 (2004).

[19] O. Morsch, J. H. Müller, M. Cristiani, D. Ciampini, and E. Arimondo, Bloch Oscillations and Mean-Field Effects of Bose-Einstein Condensates in 1D Optical Lattices, *Phys. Rev. Lett.* **87**, 140402 (2001).

[20] M. Gustavsson, E. Haller, M. J. Mark, J. G. Danzl, G. Rojas-Kopeinig, and H.-C. Nägerl, Control of Interaction-Induced Dephasing of Bloch Oscillations, *Phys. Rev. Lett.* **100**, 080404 (2008).

[21] A. Buchleitner and A. R. Kolovsky, Interaction-Induced Decoherence of Atomic Bloch Oscillations, *Phys. Rev. Lett.* **91**, 253002 (2003).

[22] S. Walter, D. Schneble, and A. C. Durst, Bloch oscillations in lattice potentials with controlled aperiodicity, *Phys. Rev. A* **81**, 033623 (2010).

[23] L. Fallani, C. Fort, and M. Inguscio, Bose-Einstein condensates in disordered potentials, *arXiv:* **0804.2888v2 [cond-mat.dis-nn]** (2008).

[24] S. Drenkelforth, G. Kleine Büning, J. Will, T. Schulte, N. Murray, W. Ertmer, S. L., and J. J. Arlt, Damped Bloch Oscillations of Bose-Einstein Condensates in Disordered Potential Gradients, *New J. Phys.* **10**, 045027 (2008).

[25] T. Schulte, S. Drenkelforth, G. K. Büning, W. Ertmer, J. Arlt, M. Lewenstein, and L. Santos, Dynamics of Bloch oscillations in disordered lattice potentials, *Phys. Rev. A* **77**, 023610 (2008).

[26] B. Deissler, M. Zaccanti, G. Roati, C. D'Errico, M. Fattori, M. Modugno, G. Modugno, and M. Inguscio, Delocalization of a disordered bosonic system by repulsive interactions, *Nature Physics* **6**, 354 (2010).

[27] D. K. K. Lee and J. M. F. Gunn, Bosons in a random potential: condensation and screening in a dense limit, *J. Phys.: Condens. Matter* **2**, 7753 (1990).

[28] K. G. Singh and D. S. Rokhsar, Disordered bosons: Condensate and excitations, *Phys. Rev. B* **49**, 9013 (1994).

[29] C. J. Pethick and H. Smith, *Bose-Einstein Condensation in Dilute Gases, second edition* (Cambridge University Press, UK, 2008).

[30] C. G. Townsend, N. H. Edwards, C. J. Cooper, K. P. Zetie, C. J. Foot, A. M. Steane, P. Szriftgiser, H. Perrin, and J. Dalibard, Phase-space density in the magneto-optical trap, *Phys. Rev. A* **52**, 1423 (1995).

[31] W. Ketterle, D. S. Durfee, and D. M. Stamper-Kurn, Making, probing and understanding Bose-Einstein condensates, in *Proceedings Of the Interna-*

tional School of Physics Enrico Fermi, edited by M. Inguscio, S. Stringari, and C. E. Wieman pp. 67, Amsterdam, 1999, IOS Press.

[32] F. Dalfovo, S. Giorgini, L. P. Pitaevskii, and S. Stringari, Theory of Bose-Einstein condensation in trapped gases, *Rev. Mod. Phys.* **71**, 463 (1999).

[33] R. H. Reimann, *Quantum Gases in State-Dependent Optical Potentials*, Master's thesis, Stony Brook University 2009.

[34] O. Mandel, M. Greiner, A. Widera, T. Rom, T. W. Hänsch, and I. Bloch, Coherent Transport of Neutral Atoms in Spin-Dependent Optical Lattice Potentials, *Phys. Rev. Lett.* **91**, 010407 (2003).

[35] Ashcroft and Mermin, *Solid State Physics* (W. B. Saunders Company, 1976).

[36] W. Zwerger, Mott–Hubbard transition of cold atoms in optical lattices, *J. Opt. B: Quantum Semiclass. Opt.* **5**, 9 (2003).

[37] M. Modugno, C. Tozzo, and F. Dalfovo, Role of transverse excitations in the instability of Bose-Einstein condensates moving in optical lattices, *Phys. Rev. A* **70**, 043625 (2004).

[38] A. R. Kolovsky, H. J. Korsch, and E.-M. Graefe, Bloch oscillations of Bose-Einstein condensates: Quantum counterpart of dynamical instability, *Phys. Rev. A* **80**, 023617 (2009).

[39] U. Gavish and Y. Castin, Matter-Wave Localization in Disordered Cold Atom Lattices, *Phys. Rev. Lett.* **95**, 020401 (2005).

[40] B. Gadway, D. Pertot, J. Reeves, M. Vogt, and D. Schneble, Glassy behavior in a binary atomic mixture, *arXiv:* **1107.2428v1 [cond-mat.quant-gas]** (2011).

[41] S. Ospelkaus, C. Ospelkaus, O. Wille, M. Succo, P. Ernst, K. Sengstock, and K. Bongs, Localization of Bosonic Atoms by Fermionic Impurities in a Three-Dimensional Optical Lattice, *Phys. Rev. Lett.* **96**, 180403 (2006).

[42] P. W. Anderson, Absence of Diffusion in Certain Random Lattices, *Phys. Rev.* **109**, 1492 (1958).

[43] L. Fallani, J. E. Lye, V. Guarrera, C. Fort, and M. Inguscio, Ultracold Atoms in a Disordered Crystal of Light: Towards a Bose Glass, *Phys. Rev. Lett.* **98**, 130404 (2007).

[44] D. Boiron, C. Mennerat-Robilliard, J.-M. Fournier, L. Guidoni, C. Salomon, and G. Grynberg, Trapping and cooling cesium atoms in a speckle field, *Eur. Phys. J. D* **7**, 373 (1999).

[45] P. Horak, J.-Y. Courtois, and G. Grynberg, Atom cooling and trapping by disorder, *Phys. Rev. A* **58**, 3953 (1998).

[46] H. Gimperlein, S. Wessel, J. Schmiedmayer, and L. Santos, Ultracold Atoms in Optical Lattices with Random On-Site Interactions, *Phys. Rev. Lett.* **95**, 170401 (2005).

[47] D.-W. Wang, M. D. Lukin, and E. Demler, Disordered Bose-Einstein Condensates in Quasi-One-Dimensional Magnetic Microtraps, *Phys. Rev. Lett.* **92**, 076802 (2004).

[48] W. C. Stwalley, Stability of Spin-Aligned Hydrogen at Low Temperatures and High Magnetic Fields: New Field-Dependent Scattering Resonances and Predissociations, *Phys. Rev. Lett.* **37**, 1628 (1976).

[49] S. Inouye, M. R. Andrews, J. Stenger, H.-J. Miesner, D. M. Stamper-Kurn, and W. Ketterle, Observation of Feshbach resonances in a Bose–Einstein condensate, *Nature* **392**, 151 (1998).

[50] D. Pertot, D. Greif, S. Albert, B. Gadway, and D. Schneble, Versatile transporter apparatus for experiments with optically trapped Bose–Einstein condensates, *J. Phys. B: At. Mol. Opt. Phys.* **42**, 215305 (2009).

[51] S. G. Albert, *Cooling, Trapping, and Transport of Atom Clouds in a New BEC Apparatus*, Master's thesis, Stony Brook University 2007.

[52] D. G. Greif, *Evaporative cooling and Bose-Einstein Condensation of Rb-87 in a moving-coil TOP trap geometry*, Master's thesis, Stony Brook University 2007.

[53] D. E. Sproles, *Laser Spectroscopy and Magneto-Optical Trapping of Rubidium Atoms*, Master's thesis, Stony Brook University 2008.

[54] H. J. Metcalf and P. van der Straten, *Laser Cooling and Trapping* (Springer, Berlin, 1999).

[55] *Daniel A. Steck, "Rubidium 87 D Line Data," available online at http://steck.us/alkalidata (revision 2.0.1, 2 May 2008).*

[56] P. L. Kapitza and P. A. M. Dirac, The reflection of electrons from standing light waves, *Mathematical Proceedings of the Cambridge Philosophical Society* **29**, 297 (1933).

[57] B. Gadway, D. Pertot, R. Reimann, M. G. Cohen, and D. Schneble, Analysis of Kapitza-Dirac diffraction patterns beyond the Raman-Nath regime, *Optics Express, Vol. 17, Issue 21, pp. 19173-19180 (2009)* **17**, 19173 (2009).

[58] P. W. Milonni and J. H. Eberly, *Laser Physics* (John Wiley & Sons, Inc., Hoboken, New Jersey, 2010).

[59] D. Witthaut, M. Werder, S. Mossmann, and H. J. Korsch, Bloch oscillations of Bose-Einstein condensates: Breakdown and revival, *Phys. Rev. E* **71**, 036625 (2005).